Research Square

Preprints are preliminary reports that have not undergone peer review.
They should not be considered conclusive, used to inform clinical practice,
or referenced by the media as validated information.

Optimized LQR Controller Design for Control of MIMO Systems based on Real Coded Genetic Algorithm

Sumit Kumar Pandey

skpdmk@gmail.com

Jharkhand Rai University

Research Article

Keywords: MIMO, TRMS, RCGA, LQR

Posted Date: November 11th, 2026

DOI: https://doi.org/10.21203/rs.3.rs-10794040/v1

License: This work is licensed under a Creative Commons Attribution 4.0 International License.
Read Full License

Additional Declarations: No competing interests reported.

Optimized LQR Controller Design for Control of MIMO Systems based on Real Coded Genetic Algorithm

Sumit Kumar Pandey
Faculty of Science and Engineering, Jharkhand Rai University, Ranchi, India
skpdmk@gmail.com

Abstract: In this work, an optimal linear quadratic regulator (LQR) based controller is designed to control the twin rotor MIMO system (TRMS). To achieve the best possible system performance, the settings of the LQR controller are improved by the use of a real coded genetic algorithm (RCGA). The control of TRMS is a challenging task due to its strong nonlinear characteristics and high cross-coupling effects. This work additionally tests the robustness of the developed controller using the multi-channel output gain and delay margin. This work also tests the developed controller's ability to reject disturbances. The plotted output responses show the efficacy of the designed controller.

Keywords: MIMO, TRMS, RCGA, LQR

1. Introduction

Any multi-input multi-output (MIMO) complex system can be a combination of a large number of inputs and outputs that are intricately connected. It makes the structure of the system complex and this complex architecture of a MIMO system makes control strategy more difficult. In the conventional control theory transfer function approach is mainly considered to design the controller for the MIMO system. Whereas the state space approach is a modern technique that can be extended to control single-input single-output (SISO) plants to MIMO plant. Since the state space approach works in the time domain hence it also helpful for non-linear systems. In this system, the state is defined as the absolute minimum set of parameters or variables required to determine the behaviour of the system. Since the state space approach is advantageous to MIMO systems and the number of axes in the state space equals the number of state variables meaning that the state space is the Euclidian space with the variables on the axes being the state variables. Some scholars have expressed interest in working on the MIMO system's state space in recent years.

In [1] linear state feedback control design method is applied to control the twin rotor MIMO system (TRMS). The Kalman filter and state observer are used to estimate the unknown states of the plant in this work. TRMS is controlled by a non-linear state observer in [2-3], where external disturbances are tackled through non-linear disturbances and friction controller. Chebyshev neural network is also taken into account to design the controller in this work. TRMS is intended to be controlled by an observer-based optimum state feedback controller in [4], and simulation results exhibit the performance of the designed controller. The extended Kalman observer-based robust proportional integral derivative (PID) controller is intended to regulate TRMS [5]. Second order sliding mode controller is designed to control TRMS in [6]. To attain the intended performance, integral-based sliding surfaces are used. The purpose of a robust PID controller is to regulate TRMS when actuator nonlinearity exists. In this study, a PID controller is designed using an optimization approach. [7]. Different optimization techniques are applied to tune the PID control for TRMS in [8]. The performance of different techniques is compared to show the efficacy of the proposed method. TRMS is intended to be controlled by an H-infinity controller based on linear matrix inequality in [9]. In this, the controller is designed to consider different inequality constraints. TRMS is intended to be controlled by a lower-order observer-based controller [10] and designed method is successfully implemented in the experimental setup. The experimental results demonstrate the superiority

of the proposed method. A robust PID-based controller is intended to regulate TRMS and is put into practice on an experimental TRMS configuration [11].
The ideal controller is made to regulate the power system's load frequency [12]. PI and PID controllers are used in this work to get the optimum performance. A particle swarm optimization-based PID controller is utilized to regulate the power system's LFC [13]. Two areas of interconnected power systems are considered for the implementation of the designed controller. Multi-area interconnected power system is controlled through the model predictive control technique [14]. An optimal Controller based on the linear quadratic Gaussian (LQG) method is applied to control the wind turbine power plant [15]. In this paper, the limitation of the proposed method is also discussed in detail. [16-17] depict the full order observer and LQG-based control method to control the load frequency of the single area power system. The performance of the proposed method is also compared. In [18] teaching learning-based optimization (TLBO) method is used to adjust the PID controller of fractional order for controlling the electromechanical system. In [19], the TRMS is controlled by a PID controller that is based on a pre-searched genetic algorithm. Here, four independent optimization techniques are applied to tune the PID controller to control the TRMS system. The performance of two different optimization methods is compared in [20-22]. In this, particle swarm optimization (PSO) and GA are compared through the output responses of the plant. A hybrid method of optimization is proposed in [23] for economical load dispatch. Here, GA and PSO are combined to achieve the optimum performance of the system. The remainder of the paper is structured so that the next section describes the mathematical modelling of the TRMS followed by the optimal controller design in section 3. Section 4 consists of the result and discussion part of the paper, and the conclusion is narrated in section 5.

2. Twin rotor MIMO System (TRMS)

TRMS is regarded as the MIMO system's real-time example in this work. It is an aerodynamical model or laboratory prototype of a helicopter. This work examines a system with two degrees of freedom (DOF) and takes into account the consequences of cross-coupling. The vertical and horizontal propeller thrust is produced by the main and tail rotors of the TRMS. The lifting force generated by the main rotor enables the beam to ascend vertically and rotate around the pitch axis. Alternatively, the tail rotor can be used to rotate the beam around the yaw axis to the left or right. The beam's condition is characterized by four process factors. Two additional state variables are the rotor angular velocities, which are measured by optical encoders positioned at the pivot, and the horizontal and vertical angles, which are detected by tacho-generators attached to the driving DC motors. In recent times, a lot of research has been done on the creation of various methods for managing the flight of aerial vehicles, like UAVs and helicopters. The complex nonlinear interactions between many variables, also due to some states not being accessible for measurement, make modelling the dynamics of air vehicles extremely difficult [1].
TRMS has the ability to rotate both vertically and horizontally. The TRMS travels upward along the pitch axis as a result of the lift force produced by the main rotor. While the TRMS rotates around the yaw axis as a result of the tail rotor. Although TRMS and helicopters are similar, they differ significantly in certain important ways. In a helicopter, this is accomplished by altering the angle of attack, while in a TRMS, it is accomplished by altering the rotor speed. Numerous methodologies have been employed to facilitate the modelling and control of TRMS.
The characteristics of the TRMS that make it challenging to model and regulate include the high degree of non-linearity and cross-coupling between variables. The main rotor and tail rotor are the primary sources of the cross-coupling. The TRMS must have an adequate control mechanism installed in order for it to function with extremely dependable performance [11].

Above all, the controller needs to be able to handle the system's high levels of cross-coupling and non-linearity. Feedback Instruments provides a laboratory setup called the TRMS that is used to evaluate new controllers. In TRMS two DC motors are in charge of the main and tail rotors. A desktop PC's installed DAC card operates the DC motors. Commands are sent from the controller, which is created with SIMULINK and MATLAB, to the DAC card. The real-time windows target allows for MATLAB-based real-time TRMS control.

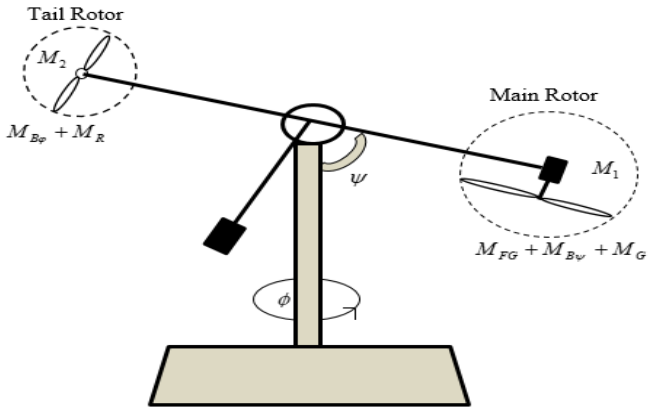


Fig. 1- TRMS Setup

The non-linear equations are obtained in accordance with Fig. 1, and the different parameters are listed in [8], thus

$$I_1 \cdot \dot{\Psi} = M_1 - M_{FG} - M_{B\emptyset} - M_G \quad (1)$$

where M_1 is the rotor-induced nonlinearity, which can be calculated as a second-order polynomial, and which induces torque in the TRMS.

$$M_1 = a_1 \cdot \tau_1^2 + b_1 \cdot \tau_1 \quad (2)$$

The gravitational torque about the pivot point in Fig. 1 is produced by the weight of the helicopter and is explained by

$$M_{FG} = m_g \cdot sin\Psi \ . \quad (3)$$

The following formula can be used to measure the frictional torque,

$$M_{B\Psi} = B_{1\Psi} \cdot \dot{\Psi} + B_{2\Psi} \cdot sign(\dot{\Psi}) \ . \quad (4)$$

The gyroscopic torque is caused by the coriolis force. The moving main rotor's change in azimuth position results in this torque, which may be expressed by the following Eq. (5).

$$M_G = K_{gy} \cdot M_1 \cdot \dot{\emptyset} \cdot \dot{cos}\Psi \ . \quad (5)$$

In this case, first-order transfer functions are the motor and the electrical control circuit. This is how the motor momentum is defined in the Laplace domain,

$$\tau_1 = \frac{K_1}{T_{11s}+T_{10}} \cdot u_1 \ . \quad (6)$$

A comparable formula is created for motion in the horizontal plane. The following equation, Equation 7, describes the net torques generated in horizontal plane motion

$$I_2 \cdot \ddot{\emptyset} = M_2 - M_{B\emptyset} - M_R \quad (7)$$

where M_2 is a nonlinear static feature that is comparable to the main rotor

$$M_2 = a_2 \cdot \tau_2^2 + b_2 \cdot \tau_2. \quad (8)$$

The main rotor dynamics and frictional torque are calculated simultaneously

$$M_{B\Psi} = B_{1\emptyset} \cdot \dot{\Psi} + B_{2\emptyset} \cdot sign(\dot{\Psi}). \quad (9)$$

Equation (1) describes the cross-reaction momentum (MR), which is calculated using the first-order transfer function

$$M_R = \frac{K_c \cdot (T_{0s}+1)}{T_{ps}+1} \cdot \tau_1. \quad (10)$$

Once more the following formula is used to calculate the first order transfer function for the D.C. motor with electrical circuit,

$$\tau_2 = \frac{k_2}{T_{21}s+T_{20}} \cdot u_2 \ . \tag{11}$$

The origin is taken into account as an equilibrium point while linearizing the nonlinear equations of the TRMS. The state and output vectors are indicated as $X = [\Psi \quad \dot{\Psi} \quad \emptyset \quad \dot{\emptyset} \quad \tau_1 \quad \tau_2 \quad M_R]^{\mathrm{T}}$ and $Y = [\Psi \quad \emptyset]^{\mathrm{T}}$. The linearized model can be written as $\dot{x} = Ax + Bu$ and $y = Cx + Du$ in which A, B, and C are the system, input and output matrices, respectively

$$\mathrm{A}=\begin{bmatrix} -0.8333 & 0 & 0 & 0 & 0 & 0 & 0 \\ 0 & 0 & 1 & 0 & 0 & 0 & 0 \\ 1.246 & -4.706 & -0.088 & 0 & 0 & 0 & 0 \\ 0 & 0 & 0 & -1 & 0 & 0 & 0 \\ 0 & 0 & 0 & 0 & 0 & 1 & 0 \\ 1.482 & 0 & 0 & 3.6 & 0 & -5 & 18.75 \\ -0.016 & 0 & 0 & 0 & 0 & 0 & -0.5 \end{bmatrix}, \mathrm{B}=\begin{bmatrix} 1 & 0 \\ 0 & 0 \\ 0 & 0 \\ 0 & 1 \\ 0 & 0 \\ 0 & 0 \\ 0 & 0 \end{bmatrix},$$

$$\mathrm{C} = \begin{bmatrix} 0 & 1 & 0 & 0 & 0 & 0 & 0 \\ 0 & 0 & 0 & 0 & 1 & 0 & 0 \end{bmatrix}.$$

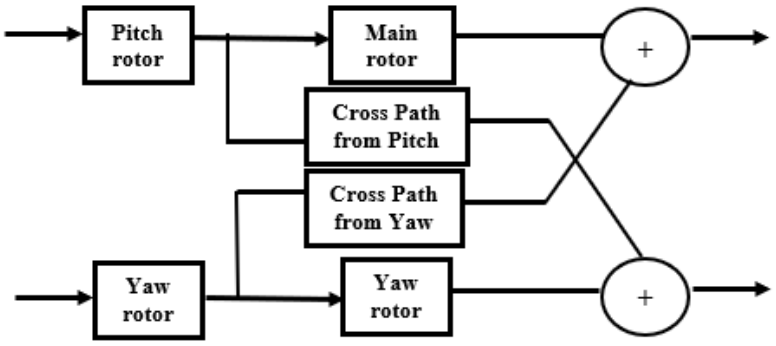


Fig. 2 - TRMS block diagram

3. Optimized LQR Controller Design

In actuality, LQR is an ideal controller. Finding the State Variable Feedback (SVFB) gain, or K, that minimizes the performance index J is aim of optimal design. An optimum controller is employed in a MIMO system because there are too many parameters [24]. Even for MIMO systems, the optimal controller technique offers a means of determining all design parameters. A trial-and-error process is also employed in the pole placement technique to ascertain the pole placements necessary for the system to operate satisfactorily. Therefore, the system's performance objective is directly formulated and the optimal controller obtains a predefined response. Additionally, optimum control minimizes the time and cost associated with system design [25-29].

The design engineer chooses the two matrices in an LQR: Q, an $n \times n$ square symmetric matrix also known as the state weighting matrix, and R, a $m \times m$ square symmetric matrix also known as the cost control matrix. The response of the closed-loop system will vary depending on how these design parameters are chosen. Choosing Q large generally means that the state $X(t)$ must be reduced in order to maintain J small. In contrast, choosing R big necessitates a smaller control input $u(t)$ in order to maintain J small. This indicates that as Q increases, the closed-loop system matrix $A_f = (A - BK)$ poles often move farther left in the s-plane, accelerating the state's decay to zero. higher R, on the other hand, indicates that less control effort is exerted, which often results in slower poles and higher state $X(t)$ values. Selecting R as positive definite

and Q as positive semi-definite is the optimal choice. For any value of $u(t)$, the scalar quantity $u^T Ru$ is always positive at time t, and for every function $X(t)$, the scalar number $X^T QX$ is either positive or zero at time t. This ensures that J has a precise definition. When it comes to eigenvalues, Q should have non-negative eigenvalues and R should have positive eigenvalues. In the event that both matrices are chosen diagonally, all of R's entries must be positive, and all of Q's entries should be positive with perhaps a few zeros on their diagonal. Then, take note that R is invertible. Fig. 3 depicts the description of the plant's control input.

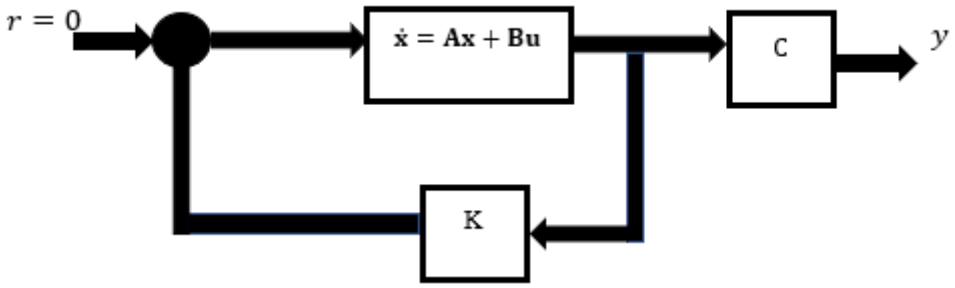


Fig. 3 - Block diagram for LQR

$$u(t) = -K(t)X(t) \tag{12}$$

$u^T(t)R(t)u(t)$ is the control energy in this case, where $R(t)$is the square matrix, commonly known as the control cost matrix.

In this instance, the control input is linear. Because there is a quadratic function of $u(t)$ in the equation, the formula for the control energy is in quadratic form. With Q(t) being a square symmetric matrix known as the state weighting matrix, the transient energy may be written as $X^T(t)Q(t)X(t)$. Therefore, the intended purpose is,

$$J_{(t,t_f)} = \int_t^{tf} \{x^T\, Q(t)x(t) + u^T R(t)u(t)\}dt \tag{13}$$

where, respectively, t and t_f represent the initial and end times. The primary goal here is to select an ideal value for the gain matrix $K(t)$, hence minimizing the objective function as defined by Eq. 13. By taking into account Eqs. (12) and (13)

$$\dot{X} = \big(A - BK(t)\big)X(t)\,. \tag{14}$$

Let's look at the near loop state dynamics matrix $A_f = A - BK(t)$. The following is a written solution to equation (14)

$$x(t) = \theta_k(t, t_0)x(t_0) \tag{15}$$

where the state transition matrix of the closed loop system is denoted by, $\theta_K(t, t_0)$. Now, replacing eqn. 15 with eqn. 13,

$$J_{(t,t_f)}=\int_t^{t_f}(x^T(t)\theta_k\,(\tau,t)(Q(\tau) + K^T(\tau)R(\tau)K(\tau))\theta_k(\tau,t)x(t)d\tau\,. \tag{16}$$

This might be expressed as

$$J_{(t,t_f)} = X^T M\big(t, t_f\big)X(t)\,. \tag{17}$$

Putting equations (15) and (16) together,

$$J_{(t,t_f)} = \int_t^{t_f}(x^T(\tau)\big(Q(\tau) + K^T(\tau)R(\tau)K(\tau)\big)x(\tau)d\tau\,. \tag{18}$$

Now differentiating and partially differentiating equation (18) with regard to time yields the following.

$$-\frac{\partial M(t,t_f)}{\partial t} = A_k(t)M\big(t, t_f\big) + A_k^T(t)M\big(t, t_f\big) + (Q(t) + K^T(t)R(t)K(t)) \tag{19}$$

The matrix Riccati equation for a finite time period is described by the equation above. By solving equation 19, the optimal control gain matrix $K(t)$ may be found

$$K(t) = R^{-1}(t)B^{T}(T)M \quad . \tag{20}$$

3.1 Real-coded genetic algorithm (RCGA)

Genetic algorithms (G.A.) were first described and formalized by Holland [19-20], who also extended the concept to encompass functional optimization. It attempts to solve an optimization problem with cost function $f(x)$ where $x = [x_1, x_2, \ldots., x_n]$ is the N −dimensional vector of optimization parameters, by modeling the processes of natural selection and evolution. Chromosomes and genes are the fundamental components of the binary G.A. Using the conventional binary G.A., the optimization parameters are encoded into a binary code string. Within G.A., a gene is binary data. Compared to its binary-coded sibling, RCGA has many advantages when working with vast, continuous search areas and high numerical precision requirements. The length of the answer to the problem remains proportionate to the chromosome's size with each gene in RCGA representing a variable in the problem.

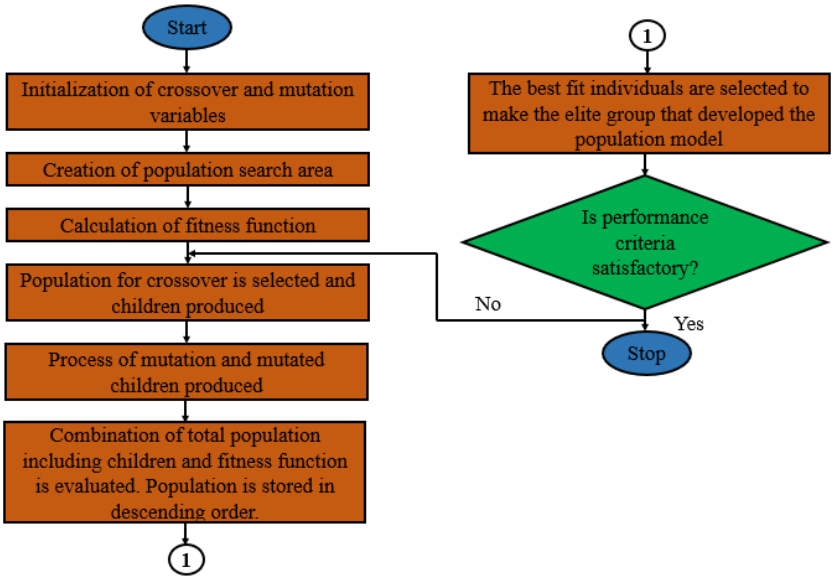


Fig. 4 - Flow chart of RCGA algorithm

As a result, unlike the binary implementation, RCGA may handle enormous domains without compromising precision (assuming a fixed length of the chromosomes). Additionally, to enhance the performance of GA, RCGA provides for the integration of domain knowledge and the ability to tune solutions locally. Fig. 4 displays the RCGA optimization flow chart. Crossover, mutation, and selection (or reproduction) are the three genetic processes. The algorithm's primary component is them. By choosing healthy chromosomes based on their fitness values, the selection operator creates the mating pool, a transient population. This can be accomplished with a variety of strategies, but the most widely used ones include the roulette wheel, ranking, and stochastic binary tournament selection. It is the selection operator's fault that the method converges. The primary search tool is the crossover operator. In the mating pool, chromosomes are joined in pairs, and potential children are created by crossing over the mated pairs with a likelihood. Numerous crossover types have been created, including random multipoint, two-point, one-point, and point crossover. Following crossover, there is a chance that some of the candidate offspring's genes will be inverted. The mutation operation is this. In order to ensure population diversity and avoid early convergence, the mutation operator is included. Thus, a new population is created.

3.2 Steps of Controller Design

Step 1. The system to which controller is design is to be written in state space form using the equation $\dot{x} = Ax + Bu$ and $y = Cx$ where A is the system matrix $B$is the input matrix and $C$is the output matrix of the plant.

Step 2. Next the compensated system is formed following the equation $\dot{x} = A_f x + Bu$ and $y = Cx$ where A_f is calculated as $A_f = A - BK$ in which K is the state feedback gain matrix.

Step 3. The gain matrix K is calculated through LQR, the method where Q & R are weighting matrices in which the performance of the controller is dependent and the value of $K$is calculated.

Step 4. The value of Q & R matrix is calculated using the RCGA method, which satisfactorily fulfils the objective functions as denoted in equation (16).
Taking the closed loop system's asymptotic stability into account and the values of Q and R as written below are obtained through proposed technique,

$$Q = \begin{bmatrix} 69 & 0 & 0 & 0 & 0 & 0 & 0 \\ 0 & 69 & 0 & 0 & 0 & 0 & 0 \\ 0 & 0 & 69 & 0 & 0 & 0 & 0 \\ 0 & 0 & 0 & 50 & 0 & 0 & 0 \\ 0 & 0 & 0 & 0 & 50 & 0 & 0 \\ 0 & 0 & 0 & 0 & 0 & 169 & 0 \\ 0 & 0 & 0 & 0 & 0 & 0 & 150 \end{bmatrix}, R = \begin{bmatrix} 100 & 0 \\ 0 & 30 \end{bmatrix}.$$

The gain matrix obtained from these Q and R matrices:

$$K = \begin{bmatrix} -0.078 & 0.07 & 0.73 & -0.61 & 1.28 & 0.26 & -0.54 \\ 0.2 & 0.09 & 0.01 & 0.54 & 0.91 & 0.18 & 4.04 \end{bmatrix}.$$

4. Results and Discussion

4.1 Time domain performance:

The controller created in the preceding section is also put to the test in simulation for its time-domain performance. The step response for the main rotor is displayed in Figs. 5(a) and (b), respectively.

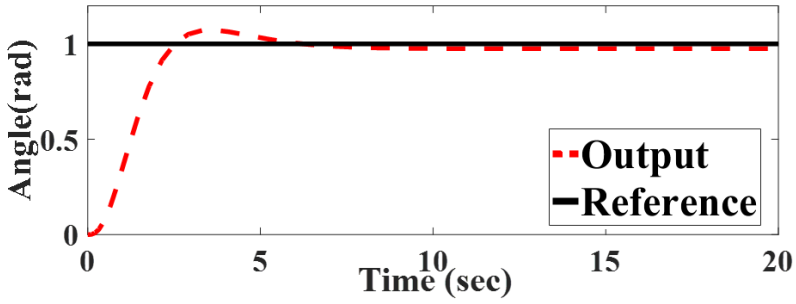


Fig. 5 (a) - Simulated step response of RGA-based decoupled TRMS main (pitch) rotor

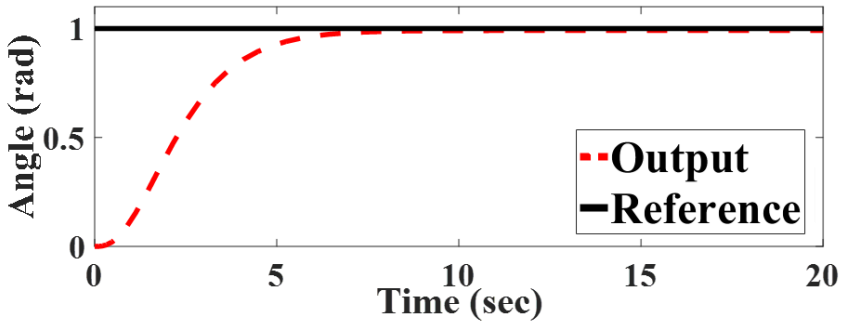


Fig. 5 (b) - Simulated step response of RGA-based decoupled TRMS tail (yaw) rotor

4.2 Determination of multi-channel output gain margin (MOGM)

The simulation results confirm that the system stays stable throughout the variable range of gain (δ) of [-0.26, 0.10]. Fig. 6 (a) and (b) portrayed the simulated step response of the main and tail rotor for $\delta = -0.26, \delta = 0.10$ respectively.

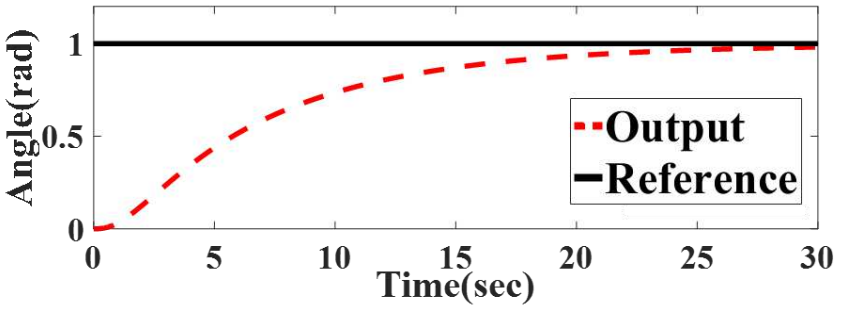


Fig. 6 (a) - Simulated step response of RGA based decoupled TRMS main (pitch) rotor with $\delta = -0.26$

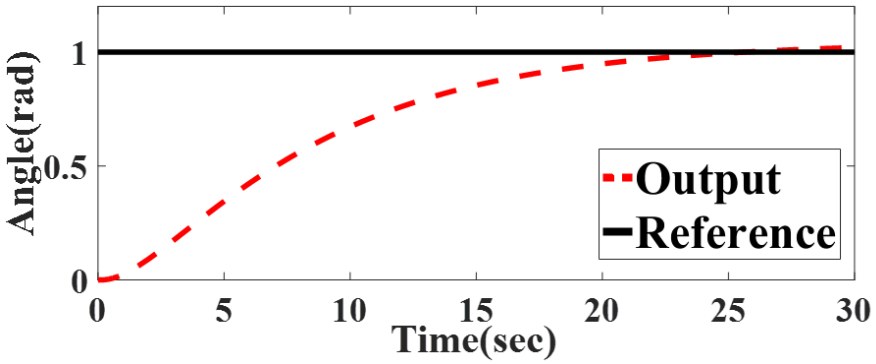


Fig. 6 (b) - Simulated step response of RGA based decoupled TRMS tail (yaw) rotor with $\delta = -0.10$

4.3 Multi-channel output delay margin (MODM)

According to Fig. 7, TRMS is shown to be stable up to a delay of $\tau_1 = 0.09$ for the main rotor and $\tau_2 = 0.14$ for the tail rotor in simulation.

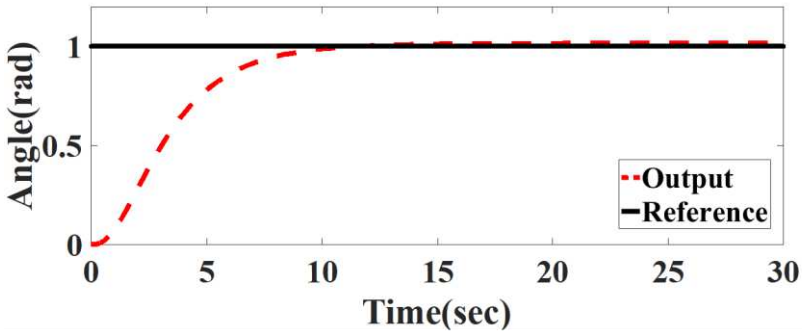


Fig. 7 (a) - Simulated step response of RGA based decoupled TRMS main (pitch) rotor with $\tau_1 = 0.09$

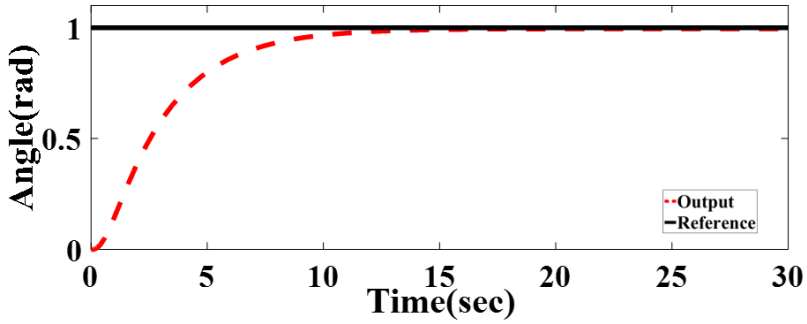


Fig. 7 (b) - Simulated step response of RGA based decoupled TRMS tail (yaw) rotor with $\tau_2 = 0.14$

4.4 Output disturbance rejection

The output disturbance rejection performance of the designed controller is verified by adding the external disturbances in the output of the plant. It is applied in such a manner that it will added at 50 seconds to the first output of the TRMS and at 70 seconds to the second output of the plant. Through the output responses it is seen that the performance of the designed controller is quite capable to eliminate the external disturbances of the plant.

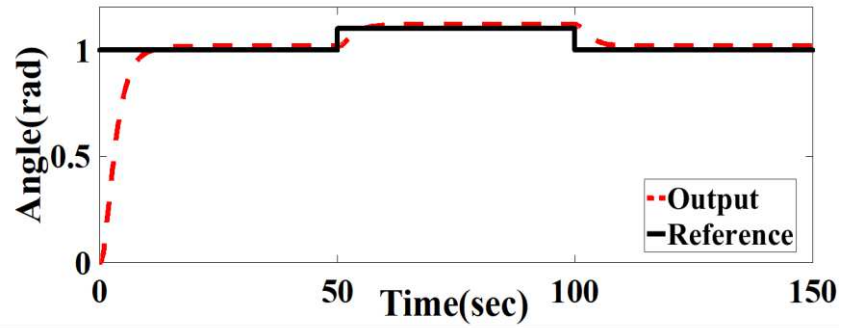


Fig.8 (a)- Main rotor step reaction (pitch angle) to output disturbance

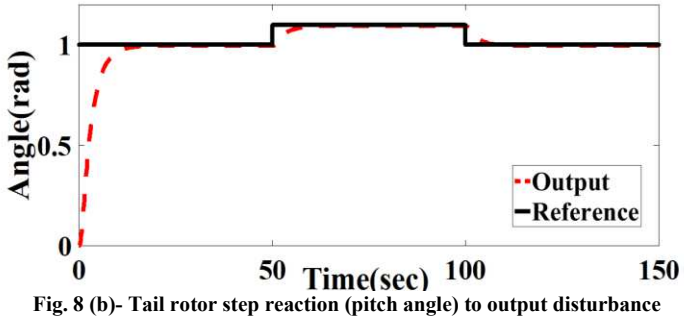


Fig. 8 (b)- Tail rotor step reaction (pitch angle) to output disturbance

5 Conclusion

This paper develops an optimal LQR) based controller for the twin rotor MIMO system (TRMS). To achieve the best possible system performance, the real coded genetic algorithm (RCGA) is used to improve the settings of the LQR controller. Because of its strong nonlinear properties and substantial cross-coupling effects, controlling TRMS is a difficult task. In this study, the multi-channel output gain margin and delay margin are also used to assess the robust performance of the developed controller. The effectiveness of the developed controller is demonstrated by the plotted output responses.

REFERENCES

1. K S Haider, K S Haider, M I Rehman, Kalman filter-based state estimation for Linearized Twin Rotor System, Frontiers of Information Technology,2011, pp.179-182.
2. B Pratap, S Purwar, Real-time implementation of nonlinear state and disturbance observer-based controller for twin rotor control system, International Journal of Automation and Control, Vol. 13, No. 4, 2019, pp. 469-497.
3. R Maiti, K D Sharma, G Sarkar, Optimal State Feedback Controller and Observer Design For Twin Rotor MIMO System, 2nd International Conference on Control, Instrumentation, Energy & Communication, 2016
4. V.S Rao, A D Rafael, M M Viviescas, Extended Kalman observer based Robust Control of 1DOF TRMS, 12th Asian Control Conference (ASCC) Kitakyusyu International Conference Center, Japan, June 9-12, 2019
5. B Pratap and S Purwar, State Observer Based Robust Feedback Linearization Controller for Twin Rotor MIMO System, IEEE International Conference on Control Applications (CCA) Part of 2012 IEEE Multi-Conference on Systems and Control,2012
6. S Mondal and C Mahanta, Second Order Sliding Mode Controller for Twin Rotor MIMO System,
7. Sumit Kumar Pandey, Jayati Dey, and Subrata Banerjee, "Design of robust PID controller for generalized deoupled TRMS with actuator non-linearity," *Journal of Systems and Control Engineering, Sage Publication*, vol.232(8), pp.971-981,2018.
8. Sumit Kumar Pandey, Jayati Dey, and Subrata Banerjee, "Design of optimal PID controller for control of twin-rotor MIMO system (TRMS)", Advances in Power and Control Engineering, *Lecture Notes in Electrical Engineering,* vol.609, pp.93-106,2019
9. Sumit Kumar Pandey, Jayati Dey, and Subrata Banerjee, "Design of H-infinity controller for twin rotor MIMO System (TRMS) based on Linear Matrix Inequalities," *"Lecture Notes in Electrical Engineering", Springer Publication,* vol.475, pp. 465-473, 2018
10. Bidisha, Jayati Dey & Sumit Kumar Pandey, "Design of optimal controller for TRMS based on reduced order state observer", 4th International Conference on Electronics, Materials Engineering & Nano-Technology (IEMEN-Tech), 2020.
11. Sumit Kumar Pandey, Jayati Dey, and Subrata Banerjee, "Design and Real-time Implementation of Robust PID Controller for Twin Rotor MIMO System (TRMS) based on Kharitonov's Theorem", Proc. of 1st IEEE International Conference on Power Electronics. Intelligent Control and Energy Systems, ICPEICES-2016
12. Devashish and Kusum Verma, Optimal Load Frequency Control of Interconnected Two Area Non-Reheat Thermal- Thermal Power System, 3rd International Conference for Emerging Technology (INCET) Belgaum, India. May 27-29, 2022
13. N E Y Kouba, M Menaa, M Hasni, B Boussahoua, and M Boudour, Optimal Load Frequency Control in Interconnected Power System Using PID Controller Based on Particle Swarm Optimization
14. A. B. Kunya, M. Argin, S. Kucuksari, Optimal Load Frequency Control of Multi-Area Power System Considering Incremental Control Action
15. A Kalbat, Linear Quadratic Gaussian (LQG) Control of Wind Turbines
16. Sumit Kumar Pandey, Prity Gupta & Shashank Shekhar Dwivedi, "Full order observer-based load frequency control of Single Area Power System", 12th IEEE International Conference on Computational Intelligence and Communication Networks, Birla Institute Bhimtal, Nainital, India, 2020
17. Sumit Kumar Pandey and Nusrat Jahan, "Load Frequency Control of Single Area Power System using LQG Controller",2nd IEEE International Conference on Innovative Practices in Technology and Management (ICIPTM), Amity University, India, 2022
18. Bishal Dey, Sumit Kumar Pandey & Anindita Sengupta "TLBO Optimized LQR based FOPID Controller" 3rd IEEE International Conference on Smart Technologies for Power, Energy and Control, (STPEC), 2023

19. J G Juang, M T Huang and W K Liu, PID Control Using Pre searched Genetic Algorithms for a MIMO System, IEEE Transactions on Systems, Man, and Cybernetics - PART C: Applications and Reviews, vol. 38, no. 5, 2008, pp 716-727.
20. R Rajendra, D K Pratihar, Particle Swarm Optimization Algorithm vs Genetic Algorithm to Develop Integrated Scheme for Obtaining Optimal Mechanical Structure and Adaptive Controller of a Robot, Intelligent Control and Automation, 2011, 2, 430-449
21. R Hassan, B Cohanim and O d Weck, A Comparison of Particle Swarm Optimization and the Genetic Algorithm, American Institute of Aeronautics and Astronautics
22. M younes, F benhamida, Genetic Algorithm-Particle Swarm Optimization (GA-PSO) for Economic Load Dispatch, Przegląd Elektrotechniczny (Electrical Review, 2011, 369-372.
23. C C Chiu, Y T Cheng and C W Chang, Comparison of Particle Swarm Optimization and Genetic Algorithm for the Path Loss Reduction in an Urban Area, Journal of Applied Science and Engineering, Vol. 15, No. 4, 2012, pp. 371-380.
24. P. Falb, & W. Wolovich , Decoupling in the design and synthesis of multivariable control systems. IEEE Transactions on Automatic Control, 1967, 12(6), 651–659.
25. V. Sankaran, & M.D. Srinath, Decoupling of linear discrete-time systems by state variable feedback. Journal of Mathematical Analysis and Applications, 1972, 39, 338–345.
26. S. K. Pandey, Stability Analysis of TRMS Using Optimal Control Technique, IEEE International Conference on Computing, Power and Communication Technologies (IC2PCT), Greater Noida, India, 2024, pp. 870-873.
27. S. K. Pandey and M. Haddad, Optimal Controller Design for Load Frequency Control of Two Area Power System,4th International Conference on Innovative Practices in Technology and Management (ICIPTM), Noida, India, 2024, pp. 1-6,
28. A. Govind, S. Selva Kumar, A Comparative Study of Controllers for QUANSER QUBE Servo 2 Rotary Inverted Pendulum System, In: Sengodan, T., Murugappan, M., Misra, S. (eds) Advances in Electrical and Computer Technologies. Lecture Notes in Electrical Engineering, vol 672. Springer, Singapore.2020.
29. S R Adarsh and S Selvakumar, Model identification and control of prosthetic leg, Journal of Physics: Conference Series,2020.